0026-895X/03/6301-26–35$7.00
MOLECULAR PHARMACOLOGY
Copyright © 2003 The American Society for Pharmacology and Experimental Therapeutics
Mol Pharmacol 63:26–35, 2003

Vol. 63, No. 1
1725/1033882
Printed in U.S.A.

Chemical Synthesis of MT1 and MT7 Muscarinic Toxins: Critical Role of Arg-34 in Their Interaction with M_1 Muscarinic Receptor

GILLES MOURIER, SÉBASTIEN DUTERTRE, CAROLE FRUCHART-GAILLARD, ANDRÉ MÉNEZ, and DENIS SERVENT

Commissariat à l'Energie Atomique, Département d'Ingénierie et d'Etude des Protéines, Gif-sur-Yvette, France

Received March 8, 2002; accepted October 10, 2002

This article is available online at http://molpharm.aspetjournals.org

ABSTRACT

Two muscarinic toxins, MT1 and MT7, were obtained by one-step solid-phase synthesis using the 9-fluorenylmethoxycarbonyl-based method. The synthetic and natural toxins, isolated from the snake venom or recombinantly expressed, display identical physicochemical properties and pharmacological profiles. High protein recovery allowed us to specify the selectivity of these toxins for various muscarinic receptor subtypes. Thus, sMT7 has a selectivity for the M_1 receptor that is at least 20,000 times that for the other subtypes. The stability of the toxin-receptor complexes indicates that sMT1 interacts reversibly with the M_1 receptor, unlike sMT7, which binds it quasi-irreversibly. The effect of the synthetic toxins on the atropine-induced [^{3}H]*N*-methylscopolamine (NMS) dissociation confirms that sMT7 targets the allosteric site on the M_1 receptor, whereas sMT1 seems interact on the orthosteric one. The great decreases in the binding potencies observed after the R34A modification in sMT1 and sMT7 toxins highlight the functional role of this conserved residue in their interactions with the M_1 receptor. Interestingly, after the R34A modification, the sMT7 toxin binds reversibly on the M_1 receptor. Furthermore, the potency of sMT7-R34A for the NMS-occupied receptor is lower compared with unmodified toxin, supporting the role of this residue in the allosteric interaction of sMT7. All these results and the different charge distributions observed at the two toxin surfaces of their structure models support the hypothesis that the two toxins recognize the M_1 receptor differently.

Several neurotoxins have been purified from the venom of African mambas (*Dendroaspis angusticeps* and *Dendroaspis polylepis*) and characterized for their specific interaction with various muscarinic receptors (for review, see Bradley, 2000; Jerusalinsky et al., 2000; Karlsson et al., 2000; Potter, 2001). These muscarinic toxins are peptides of 63 to 66 residues with four disulfide bonds and a common three-finger fold structure (Segalas et al., 1995). Despite a high sequence homology (Fig. 1), they possess notable specificity in their interactions with various muscarinic receptor subtypes and exhibit clear differences in their functional activities. For example, MT1 binds with relatively high affinity to M_1 and M_4 receptors and seems to act as a selective agonist (Jerusalinsky and Harvey, 1994; Adem and Karlsson, 1997), whereas MT7 interacts with the M_1 receptor with a 1000-fold higher affinity than with the other subtypes and binds quasi-irreversibly to an allosteric site (Max et al., 1993; Carsi and Potter, 2000; Olianas et al., 2000).

Until now, the lack of selectivity of conventional ligands for the various muscarinic receptor subtypes has explained why the physiological role of each receptor subtype in different tissues has remained unclear and has been associated with the numerous side effects of these ligands, which compromise their therapeutic potential (Eglen et al., 1999). In this context, the selectivity with which muscarinic toxins recognize some muscarinic receptors may be very useful in the identification of the type of receptor expressed in various tissues and could enable their use as potential therapeutic agents in diseases involving muscarinic receptors (Eglen et al., 1999; Bradley, 2000). However, the amount of toxin available from snake venom is often too low to allow their extensive functional characterization. Much effort has been invested in their production, and recently these toxins have been obtained either by the long and labor-intensive fragment-by-fragment chemical method (Nishiuchi et al., 2000) or by using different expression systems, such as the baculovirus vector-Sf9 insect cell expression system (Nasman et al., 2000) and yeast expression in *Pichia pastoris* (Krajewski et al., 2001). However, the expression yields in these different systems are relatively low and many steps are required to obtain enough toxin for complete functional characterization.

In this article, we describe the high recovery of muscarinic

ABBREVIATIONS: sMT1, synthetic muscarinic toxin 1; vMT1, venom purified muscarinic toxin 1; sMT7, synthetic muscarinic toxin 7; rMT7, recombinant muscarinic toxin 7; NMS, *N*-methylscopolamine; HOAT1-hydroxy-7-azabenzotriazole; Fmoc, 9-fluorenylmethoxycarbonyl; HPLC, high-performance liquid chromatography; TFA, trifluoroacetic acid; CD, circular dichroism; CHO, Chinese hamster ovary; PBS, phosphate-buffered saline; BSA, bovine serum albumin; 3D, three-dimensional.

```
Dendroaspis angusticeps
                          1        10        20        30        40        50        60
                MTX1      LTCVTSKSIFGITTENCPDGQNLCFKKWYYIVPRYSDITWGCAATCPKPTNVRETIRCCETDKCNE
                MTX2      LTCVTTKSIGGVTTEDCPAGQNVCFKRWHYVTPKNYDIIKGCAATCPKVDNN-DPIRCCGTDKCND
                MTX3 (m4-tox) LTCVTKNTIFGITTENCPAGQNLCFKRWHYVIPRYTEITRGCAATCPIPENY-DSIHCCKTDKCNE
                MTX4      LTCVTSKSIFGITTENCPDGQNLCFKKWYYIVPRYSDITWGCAATCPKPTNVRETIHCCETDKCNE
                MTX5      LTCVTSKSIFGITTEDCPDGQNLCFKRRHYVVPKIYDITRGCVATCPKPENY-DSIHCCKTDKCNE
                MTX7 (m1-tox) LTCVKSNSIWFPTSEDCPDGQNLCFKRWQYISPRMYDFTRGCAATCPKAEYR-DVINCCGTDKCNK

Dendroaspis polylepis
                MTXα      LTCVTSKSIFGITTENCPDGQNLCFKKWYYLNHRYSDITWGCAATCPKPTNVRETIHCCETDKCNE
                MTXβ      LTCVTSKSIFGITTEDCPDGQNLCFKRRHYVVPKIYDITRGCVATCPIPENY-DSIHCCKTDKCNE
                          ****   **   * * ** *** ***   *          ** ****        * ** *****
```

Fig. 1. Sequence alignment of muscarinic toxins isolated from the *D. angusticeps* and *D. polylepis* venom. The invariant residues are indicated by a star and the highly conserved positively charged residue (arginine or lysine) at position 34, studied in this article, is shown in bold type.

toxins sMT1 and sMT7 by using one-step solid-phase chemical synthesis, plus their purification and refolding procedures, and compare their physicochemical properties with those of natural toxins. To determine the pharmacological profiles of these synthetic toxins, we investigated their activity on cloned human receptors (M_1–M_4) expressed in CHO cells and examined the nature of their interactions with the M_1 subtype by analyzing their effects on [^{3}H]*N*-methyl-scopolamine (NMS) binding. We examined the stability of the toxin-receptor complexes by analyzing the rate of appearance of [^{3}H]NMS binding sites after a preincubation of the receptor with the toxins. We also synthesized modified toxins to delineate the site by which muscarinic toxins interact with their receptor targets. The functional role of the Arg-34 at the tip of the central toxin loop was highlighted in both toxins and the allosteric effect of natural and modified toxins on the dissociation of [^{3}H]NMS was studied. Finally, structural models of the two toxins were calculated and a hypothesis is proposed to explain their differential mode of interaction with muscarinic receptors.

Materials and Methods

Materials. [^{3}H]NMS (78 Ci/mmol) was from Amersham Biosciences (Orsay, France). Protected amino acid derivatives, resins, and dicyclohexylcarbodiimide were from Novabiochem (Meudon, France). 1-Hydroxy-7-azabenzotriazole (HOAT) was from Applied Biosystems (Courtaboeuf, France). Piperidine, *N*-methyl pyrrolidone, dichloromethane, methanol, and trifluoroacetic acid *tert*-butyl methyl oxide were from SDS (Peypin, France). Acetic anhydride, 2,4,6-collidine, tri-isopropylsilane, and oxidized and reduced glutathione were from Sigma-Aldrich (Saint-Quentin-Fallavier, France). Automated chain assembly was performed on a standard Applied Biosystems 433 peptide synthesizer (Applied Biosystems, Foster City, CA). Recombinant MT7 was kindly provided by Dr. E. Karlsson (Department of Clinical Neuroscience, Karolinska Institute, Huddinge, Sweden). Natural MT1 from the venom of *D. angusticeps* was from Sigma-Aldrich.

Peptide Synthesis. Assembly of the different toxins and mutants was carried out using the stepwise solid-phase method with dicyclohexylcarbodiimide/HOAT as coupling reagents and *N*-methyl pyrrolidone as solvent. Fmoc-protected amino acids were used with the following side chain protections: *t*-butyl ester (Glu, Asp), *t*-butyl ether (Ser, Thr, Tyr), trityl (Cys, His, Asn, Gln), 2,2,5,7,8-pentamethyl-chromane-6-sulfonyl (Arg), and *t*-butyloxycarbonyl (Trp). The sMT1 and sMT7 toxins and their mutants were assembled on an Fmoc-Glu(OtBu)-Wang resin (loading, 0.5 mmol/g) and Fmoc-Lys-(Boc)-Wang resin (loading, 0.55 mmol/g), respectively. The different syntheses were run on a modified version of the Applied Biosystems standard 0.1-mmol small-scale program using 0.05 mmol of each resin. This program achieves UV monitoring of the deprotection step. When the deprotection is too slow after two and/or three successive deprotections of 3 min, it automatically extends the deprotection time by 20 min and the coupling time (normal coupling, 30 min) by an extra 30 min. After each coupling, the resin was acetylated by a mixture of 5% acetic anhydride and 6% 2,4,6-collidine in dimethylformamide. At the end of the synthesis, the peptide-resins were treated with trifluoroacetic acid (9 ml), tri-isopropylsilane (0.5 ml), and 0.5 ml of distilled water. The peptides were then cleaved from the resin and the protecting groups were removed from amino acid side chains. After 2 h of incubation, the mixture was filtered in cold *tert*-butyl methyloxide and centrifuged three times. The precipitates were dissolved in a solution of 10% acetic acid and lyophilized. The toxins were purified by reversed phase HPLC using a Vydac C18 column (250 × 10 mm) with a gradient of 40 to 60% of solvent B in 40, 50, 60, and/or 90 min, (A, 0.1% TFA in H_2O; B, 60% acetonitrile and 0.1% TFA in H_2O) The flow rate was 5 ml/min and the detection was followed at 280 and 214 nm.

Disulfide Bond Formation, Protein Purification, and Physicochemical Characterization. The reduced natural and modified synthetic toxins were subjected to an oxidative reaction in 0.1 M ammonium acetate, pH 7.8, containing 1 M guanidine hydrochloride in the presence of reduced and oxidized glutathione in a molar ratio of 1/10/100 in peptide/reduced glutathione/oxidized glutathione at a peptide concentration of 0.05 mg/ml. To minimize the adsorption of protein on the vessel, the refolding was allowed to proceed in 10-ml minisorp tubes (Polylabo-Merckeurolab, Strasbourg, France). After 3 to 5 days at room temperature in the dark under argon, the pH was lowered to 3 by addition of 30% TFA and the mixture was loaded on a Vydac semipreparative column (250 × 10 mm) equilibrated with 0.1% TFA in water. The column was then submitted to the gradient previously used to purify the reduced toxin forms. The chemical properties of the synthetic (sMT7, sMT1) and natural (vMT1, rMT7) toxins were studied by chromatographic analyses. Toxins alone or in pairs (vMT1+sMT1 or rMT7+sMT7) were injected (0.5–1 μg/10 μl) on analytical reversed-phase HPLC (C18, 5 μm, 150 × 4.5 mm; Phenomenex, Torrance, CA) by means of a 40-min linear gradient of acetonitrile in 0.1% (v/v) trifluoroacetic acid from 25 to 35% at a flow rate of 1 ml/min, detection at 214 nm. The hydrolysates obtained after acid hydrolysis in a sealed vial heated at 120°C in the presence of 6N HCl for 16 h were analyzed using an Applied Biosystems model 130A automatic analyzer equipped with an online 420A derivatizer for the conversion of the free amino acid into phenyl thiocarbamoyl derivatives. Mass determinations were performed on a micromass platform II (Micromass, Altrincham, UK). The concentrations of the different toxins were evaluated spectrometrically (ϵ at 278 nm is equal to 15,470 for the reduced form and 15,970 for the oxidized form).

Circular Dichroism Analysis. CD spectra were recorded on a Jobin Yvon CD6 spectropolarimeter (Jobin Yvon, Longjumeau, France). Measurements were routinely performed at 20°C in 0.1-cm pathlength quartz cells (Hellma, Paris, France) with a peptide concentration of 5.10^{-6} M in 5 mM sodium phosphate buffer, pH 7.4. Spectra were recorded in the 186- to 260-nm wavelength range. Each spectrum represents the average of four spectra.

CHO Cells and Membrane Preparation. Profs. P. O. Couraud and A. D. Strosberg (ICGM, Paris, France) kindly provided CHO cells stably expressing the cloned human muscarinic receptors. The cells were grown in plastic Petri dishes (Falcon, Cowley, UK) that were incubated at 37°C in an atmosphere of 5% CO_2 and 95°O_2 humidified air in Ham's F12 medium precomplemented with L-glutamine and bicarbonate (Sigma) supplemented with 10% fetal calf serum and 1% penicillin/streptomycin (Sigma). At 100% confluence, the medium was removed and the cells were harvested using Versen buffer. They were washed with ice-cold phosphate buffer and centrifuged at 1700 *g* for 10 min (4°C). The pellet was suspended in ice-cold buffer (1 mM EDTA, 25 mM sodium phosphate, 5 mM $MgCl_2$, pH 7.4) and homogenized using an Potter-Elvehjem homogenizer (Fisher Scientific, Elancourt, France). The homogenate was centrifuged at 1,700*g* for 15 min (4°C). The sediment was washed, resuspended and centrifuged at 1,700*g* for 15 min (4°C). The combined supernatants were centrifuged at 35,000*g* for 30 min (4°C) and the pellet was suspended in the same buffer (0.1 ml/dish). Protein concentrations were determined according to the Lowry method using bovine serum albumin as standard. The membrane preparations were aliquoted and stored at −80°C.

Radioligand Binding Assays. The IC_{50} values of vMT1, rMT7 and synthetic sMT1 and sMT7 toxins for hM_1, hM_2, hM_3, and hM_4 receptors were determined in competition experiments with [^{3}H]NMS as tracer. The purified toxins were spectrophotometrically quantified and serially diluted in PBS-BSA (10 mM sodium phosphate, pH 7.2, 135 mM NaCl, 2.5 mM KCl, 0.1% BSA). Membrane fractions (3–4 μg of protein; 8 pmol/mg of protein) were incubated in PBS-BSA at 25°C for 1 h, with varying concentrations of toxin and [^{3}H]NMS, in a final assay volume of 300 μl. Competition experiments with sMT1 and sMT1-R34A used 1.5 nM of [^{3}H]NMS as tracer so that not more than 10% of added radioligand was bound. Thus, binding constants were determined with the Cheng-Prusoff equation (Cheng and Prusoff, 1973) using 0.1 nM as experimentally calculated affinity constant of [^{3}H]NMS on hM_1 receptor. sMT7 and sMT7-R34A toxin potencies were tested for the receptor with 0.5 nM [^{3}H]NMS. Nonspecific binding was determined in the presence of 10 μM atropine. The reaction was stopped by addition of 5 ml of ice-cold buffer (PBS) immediately followed by filtration through Whatman GF/C glass-fiber filters presoaked in 0.5% polyethylenimine. The filters were washed once again with 5 ml of ice-cold buffer (PBS), dried, and the bound radioactivity was counted by liquid scintillation counting. Each experiment was done at least three times.

Stability of the Toxin-Receptor Complexes. hM_1 membranes were incubated for 30 min with a saturating concentration of toxins, sMT7 (10 nM), sMT7-R34A (1 μM), and sMT1 (5 μM) in 100 μl of PBS-BSA. In the control experiments, no toxin was added. [^{3}H]NMS (1 nM) was added to a final volume of 6 ml, allowing monitoring of its rate of association for 5 h. The rate of appearance of binding sites for [^{3}H]NMS was taken as the rate of dissociation of the different toxins. All these experiments were repeated three times.

Allosteric Binding of Toxins. Allosteric binding of toxins for the hM_1 receptor was determined by dissociation experiments with [^{3}H]NMS as described previously (Ellis and Seidenberg, 2000). Briefly, cell membranes (amount for 10 samples) were preincubated with 1 nM [^{3}H]NMS for 45 min until equilibrium was reached. Dissociation of the radioligand was initiated by the addition of 3 μM atropine, with or without a saturating concentration of each toxin, determined from competition experiments. At different times, samples were filtered and washed, and the radioactivity retained on filters was counted.

Single time point experiments were performed to measure the inhibition of the [^{3}H]NMS dissociation by wild-type and modified toxins. These off-rate assays were previously used to estimate the affinity of allosteric agents for the [^{3}H]NMS-occupied receptor (Lazareno et al., 2000). A high concentration of hM_1 membranes (around 2 mg/ml) was incubated for 15 min with a high concentration of [^{3}H]NMS (5 nM). Then, 10-μl aliquots were added to tubes that were empty or contained 1 ml of 10 μM atropine alone and with varying concentrations of toxins. Nonspecific binding was measured by incubating 10 μl aliquots with 10 μM atropine and [^{3}H]NMS (5 nM). After 45 min of incubation (about 2.5 dissociation half-lives), the samples were filtered and rinsed two times. The data were transformed to rate constants using the formula $k_{off} = \ln(Bo/Bt)/t$, where *Bo* and *Bt* representing the [^{3}H]NMS bound initially and after *t* min of dissociation, respectively. The apparent rate constants for the dissociation of [^{3}H]NMS were determined in the presence of each concentration of toxins (k_{obs}) and divided by the true rate constant k_o determined in the presence of atropine only (Gnagey et al., 1999). The resulting number, less than 1, indicates a slower dissociation of [^{3}H]NMS in presence of the toxins compared with the control rate. The values from three experiments were fitted using a nonlinear regression analysis. Thus, the concentration inducing a half-maximal effect on [^{3}H]NMS dissociation ($EC_{50,diss}$) indicates the equilibrium dissociation constant of the toxin with the [^{3}H]NMS-occupied receptor and serves as a measure of affinity of the toxin for the allosteric site of the receptor.

Homology Modeling. The sequences of MT1 and MT7 of *D. angusticeps* were taken from the SWISS Prot databases (ID codes P81030 and P80970, respectively). Structure prediction of MT1 and MT7 was based on the 3D structure of the homologous MTX2 (TrEMBL accession number Q9PRY3) (Segalas et al., 1995). The search for sequence identity within databases was performed with the Blast program (Altschul et al., 1997). Different MTX sequences were aligned by ClustalW (Thompson et al., 1994). The 3D structure was determined by means of the Swiss-PDBViewer (ver. 3.7b2; http://www.expasy.org/spdbv) and the models were minimized with the Swiss Model (Peitsch, 1995, 1996; Guex and Peitsch, 1997). The electrostatic potentials were calculated using the computation method of Coulomb with dielectric constants of 80 and 4 for solvent and protein, respectively.

Results

Synthesis of the Wild-Type and Mutated Muscarinic Toxins. The one-step solid phase chemical synthesis of the muscarinic toxins was performed on a modified version of the Fmoc/small scale (0.1 mmol) program developed by Applied Biosystems (see *Materials and Methods*) and used successfully in the synthesis of toxin α from *Naja nigricollis*, a curaremimetic neurotoxin (Mourier et al., 2000). Here, the efficient coupling reagent HOAT (Carpino et al., 1994) was used instead of *N*-hydroxybenzotriazole to optimize the low coupling caused by steric hindrance and the increasing peptide length. The synthesis proceeded smoothly with no (sMT7, sMT7-R34A) or few minor (sMT1, sMT1-R34A) failures in the deprotection monitoring. These are located in the central part (V32-Y35) and N-terminal end (L1–S8) of the sMT1 and sMT1-R34A toxin sequences. As shown in Fig. 2, for each wild-type and modified toxin, the final TFA cleavage yielded a crude mixture in which the main component, corresponding to the reduced form of each protein, constituted 40 (sMT7), 27 (sMT1), 42 (sMT7-R34A), and 29% (sMT1-R34A) of the total reaction mixture. Optimal conditions for disulfide formation required the addition of 1 M guanidine hydrochloride to the medium to avoid formation of the precipitates and aggregates seen in abundance in the absence of this reagent (data not shown). The presence of reduced and oxidized glutathione is crucial in improving the formation of the correct species and in increasing the final oxidation yield. As shown in Fig. 2, sMT7, sMT7-R34A, sMT1, and sMT1-R34A folded in a well defined component, which eluted in the RP-HPLC profile before the reduced form. They represent,

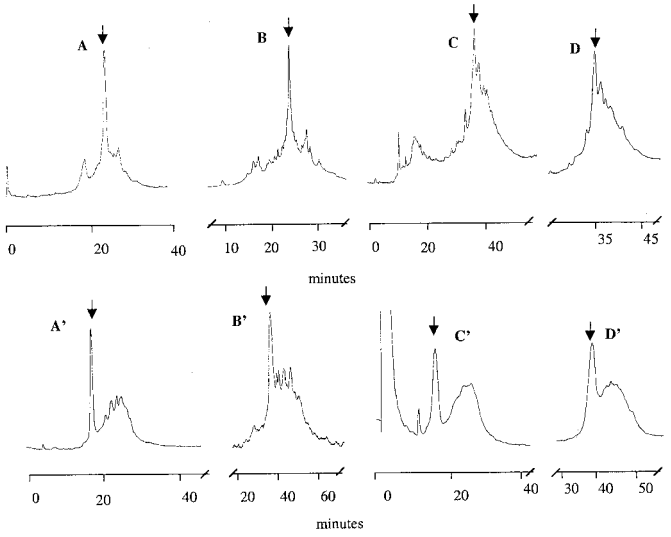

Fig. 2. Analytical HPLC profiles. Top, crude sMT7 (A), sMT7-R34A (B), sMT1 (C), and sMT1-R34A (D) after TFA deprotection. Each arrow indicates the peak corresponding to the reduced toxin. Bottom, the glutathione-mediated oxidation of the synthetic sMT7 (A′), sMT7-R34A (B′), sMT1 (C′), and sMT1-R34A (D′); each arrow indicates the peak corresponding to the refolded toxin. RP-HPLC conditions: C18 column (0.45 × 15 cm), gradient of 40 to 60% B in 40 min (A, A′, B, C′), in 50 min (D′), in 60 min (D), in 90 min (B′, C). Solvent A, 0.1% TFA in water; solvent B, 60% CH_3CN and 0.1% TFA in water at 1 ml/min. Protein detection was followed at 214 nm.

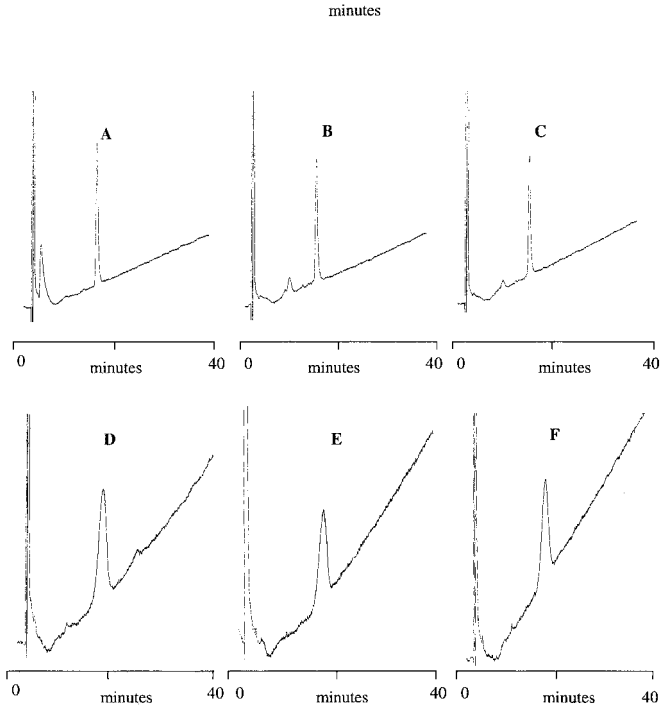

Fig. 3. Comparison of the HPLC profiles between the synthetic toxins sMT7 and sMT1 and the recombinant rMT7 and the natural vMT1. A, synthetic sMT7; B, recombinant rMT7; C, coinjection of the synthetic and recombinant MT7 (1/1); D, synthetic sMT1; E, natural vMT1; F, coinjection of the synthetic and natural MT1 (1/1). HPLC, column Phenomenex C18/300/5 (150 × 0.46 mm), eluent 25 to 35% CH_3CN in 0.1% TFA; running conditions, 40 min gradient, flow rate 1 ml/min; detection, 214 nm; injection, 0.5 to 1 μg/10 μl. (Baseline deviation is due to the high sensitivity needed for the detection.)

respectively 23% (sMT7), 18% (sMT7-R34A), 20% (sMT1), and 27% (sMT1-R34A) of the folded species present in the RP-HPLC oxidation profile. Amino acid composition and electrospray mass analysis confirmed the purity and identity of the different toxins. The masses found were 7472.0 for sMT7 (theoretical 7472.5), 7386.9 for the mutant sMT7-R34A (theoretical 7387.5), 7509.4 for sMT1 (theoretical 7508.8), and 7424.1 for the mutant sMT1-R34A (theoretical 7424.2). Finally, the purified synthetic (sMT7 and sMT1) and natural (rMT7 and vMT1) toxins, injected alone or in combination, were characterized by a single peak with identical retention time on analytical C18 reversed-phase HPLC (Fig. 3).

Secondary Structure Analyses of Wild-Type and Mutated sMT1 and sMT7. MTX2, a muscarinic toxin that belongs to the same toxin family, displays a typical three-finger fold that mostly consists of β-sheet secondary structure elements (Segalas et al., 1995). We expected that this kind of ellipticity would dominate the CD spectrum of sMT1 and sMT7 toxins. As shown in Fig. 4, our results are consistent with this assumption. sMT7 exhibits a typical β-sheet signature with pronounced maxima and minima at 196 and 214 nm, respectively. The CD spectrum of sMT1 toxin differs slightly from that of sMT7. The two bands corresponding to β-sheet secondary structure elements are still present, but the slight blue shift of the minima (i.e., 210 nm compared with the expected 212 to 216 nm) and the band at 230 nm are unclear but may reflect some local differences in the antiparallel strands between the two toxins. As shown in Fig. 4, the CD spectra of the sMT7-R34A and sMT1-R34A mutants are similar to those of the native synthetic toxins. Clearly, the mutation of the arginine in position 34 has not altered the three-dimensional structure of the two toxins.

Binding of vMT1, rMT7, sMT1, and sMT7 to Various Muscarinic Receptor Subtypes. Binding experiments using [^{3}H]NMS as tracer were performed on the one hand with vMT1, sMT1, rMT7, and sMT7 and human muscarinic receptor M_1 and on the other hand with the synthetic toxins and the other receptor subtypes (M_2–M_4) (see *Materials and Methods*). The competition binding curves are shown in Fig. 5 and the corresponding IC_{50} and apparent dissociation constants are presented in Table 1. The two synthetic toxins, sMT1 and sMT7, exhibited pharmacological properties with the M_1 receptor similar to those observed, respectively, with vMT1 and rMT7. The IC_{50} values obtained for the interaction of vMT1 and sMT1 with hM1 were 560 and 315 nM (Fig. 5A), whereas the values for rMT7 and sMT7 were 0.60 and 0.43 nM (Fig. 5B). Competition experiments with sMT7 and M_1 receptor at two different receptor concentrations (90 and 30 pM) conduce to identical IC_{50} values (data not shown). A dose-dependent inhibition was also observed for the binding of sMT1 to the M_4 receptor with an IC_{50} of 5.5 μM. Up to a concentration of 10 μM of the two synthetic toxins, no displacement of [^{3}H]NMS was observed with the other receptor subtypes (Fig. 5). Furthermore, in competition binding experiments with three different concentrations of [^{3}H]NMS (0.05, 0.5, and 5 nM), the sMT7 caused a similar dose-dependent reduction in [^{3}H]NMS binding, associated with IC_{50} values of 0.41, 0.43, and 0.56 nM, respectively (Fig. 6). Slope factors of 1.3 ± 0.1 characterized the competition binding curves shown in Fig. 6. In the equilibrium competition experiments with sMT7, the preincubation with the toxin before the addition of the [^{3}H]NMS did not modify the inhibition potency of the toxin (data not shown).

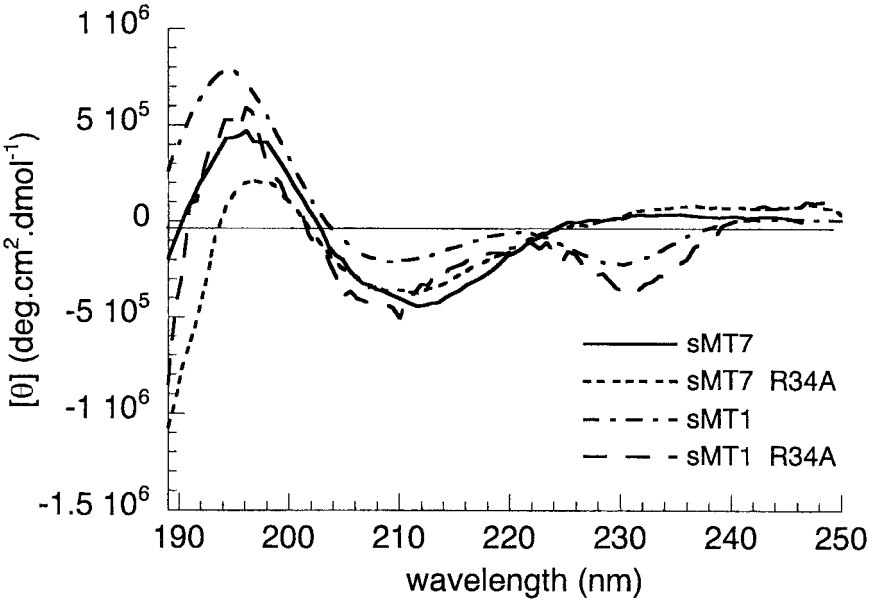

Fig. 4. Far-ultraviolet CD spectra of the different toxins and mutants. The spectra were monitored in 5 mM sodium phosphate buffer, pH 7.4, at 20°C at a peptide concentration of 5.10^{-6} M.

Role of Arg-34 in the Interaction of sMT1 and sMT7 with the hM$_1$ Receptor. As presented previously, two modified toxins were synthesized by introducing in the sequence of MT1 and MT7 an alanine in place of the arginine at position 34 at the tip of their central loop. The effect of this modification on the potency of the two toxins for the M_1 receptor was characterized in competition experiments. Figure 7 indicates that sMT7-R34A interacts with the M_1 receptor with an IC_{50} value of 45 nM, corresponding to a 105-fold affinity decrease compared with the wild-type toxin (Table 1). Slope factors of 1.3 and 1.15 are associated with the binding curves obtained with sMT7 and sMT7-R34A, respectively. Because of the drastic effect on the toxin's affinity and the use of high toxin concentration, a complete binding curve could not be obtained for the modified sMT1. Nevertheless, the sMT1-R34A apparent affinity constant could be approximated to 53 μM, a value 170 times higher than that of the wild-type toxin (Table 1). Thus, the arginine at position 34 plays important functional roles in the interaction of sMT7 and sMT1 toxins with the M_1 receptor.

Stability of the Toxin-hM1 Receptor Complexes. This property was examined by analyzing the ability of [^{3}H]NMS to bind to a receptor previously incubated with a saturating concentration of the different toxins. The rate of appearance of binding sites for [^{3}H]NMS was taken as the rate of dissociation of the different toxins. Figure 8 shows that sMT1 had no effect on the appearance of [^{3}H]NMS binding sites, indicating its reversible interaction. In contrast, preincubation of the receptor with sMT7 completely abolished the [^{3}H]NMS binding for at least 5 h, revealing that sMT7 bound quasi-irreversibly to the hM_1 receptor. When the receptor was preincubated with sMT7-R34A, the [^{3}H]NMS binding increased with time, and quasi-complete binding was reached in approximately 2 h. Thus, the irreversibility of the binding of sMT7 is affected by the R34A modification.

Orthosteric or Allosteric Binding of sMT1 and sMT7 Toxins to the M$_1$ Receptor. The ability of wild-type or modified synthetic toxins to modify the kinetics of binding of [^{3}H]NMS to the M_1 receptor was studied. In dissociation experiments, sMT7 (20 nM) decreased the rate of the atropine-induced dissociation of [^{3}H]NMS from the receptor by 7-fold. Thus, the dissociation rate constants (k_{off}) were equal to 0.037 and 0.0053 min^{-1} in the absence and presence of toxin, respectively (Fig. 9A). In contrast, sMT1 (40 μM) had no significant effect on the [^{3}H]NMS dissociation rate, as revealed by the k_{off} value of 0.033 min^{-1}. Furthermore, to determine the effect of the R34A modification on the sMT7 affinity for the NMS-occupied receptor, we calculated the concentration dependence of the effect of sMT7 and sMT7-R34A on the [^{3}H]NMS dissociation. Single time point experiments performed, as described previously (Lazareno et al., 2000), indicated IC_{50} values for the inhibition of the [^{3}H]NMS dissociation equal to 2.5 and 24 nM for sMT7 and sMT7-R34A, respectively (Fig. 9B). Slope factors of 1 characterized the competition binding curves shown in Fig. 9B. The IC_{50} values of wild-type and modified toxins for the [^{3}H]NMS-liganded receptor were calculated, confirming a significant effect of the R34A modification on the interaction of sMT7 at the allosteric binding site of the M_1 receptor.

Discussion

The muscarinic toxins of African mambas are 64- to 66-residue peptides with four disulfide bonds that are conserved throughout the family of "three-fingered" snake toxins, including muscular and neuronal neurotoxins, cardiotoxins, fasciculin, mambin, and calsiceptin (Ménez, 1998). Despite their relatively large size and high disulfide density, most of these three-fingered toxins are now accessible to chemical synthesis. We recently reported the high-yield one-step solid-phase peptide synthesis of short- and long-chain neurotoxins (Mourier et al., 2000). In the present work, we demonstrate that the two muscarinic toxins sMT7 and sMT1 can be obtained by a similar approach. The synthesis of both toxins proceeded satisfactorily, but the overall yield of sMT1 was reduced after deprotection by approximately 30% compared with sMT7.

As for short neurotoxin, the four disulfides were formed using a redox buffer and a mixture of reduced and oxidized glutathione. Significant differences between the folding pro-

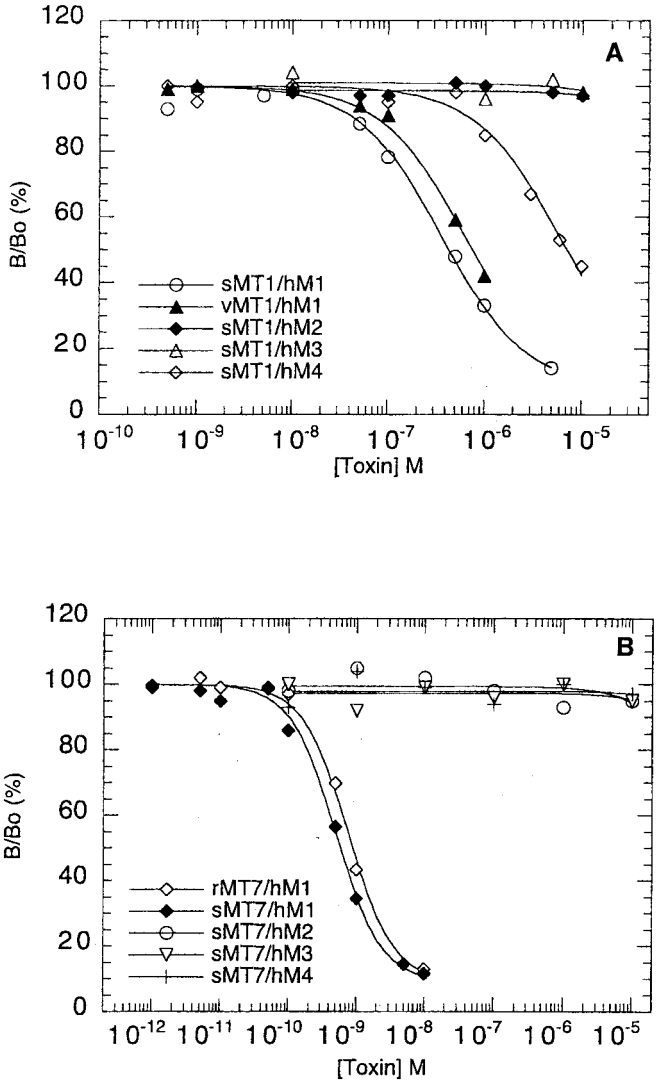

Fig. 5. Inhibition of [^{3}H]NMS binding to various muscarinic receptor subtypes by sMT1 and vMT1 (A) and sMT7 and rMT7 (B). Binding experiments were performed by incubating membrane fractions of each receptor subtype with [^{3}H]NMS and varying concentrations of toxin at 25°C for 1 h. The results are expressed as the ratio of the specific [^{3}H]NMS binding measured with (*B*) or without toxin (*Bo*) (n = 3 for each toxin).

cesses of the muscarinic toxins and those of short and long nicotinic neurotoxins were found. Thus, in the absence of a nondenaturing concentration of guanidine (0.5 or 1 M), sMT1 and sMT7 precipitate in solution and no or few folded species were detected (data not shown). Using optimized refolding conditions, a few milligrams of wild-type or modified sMT1 and sMT7 toxins were obtained in a short period of time, allowing their complete structural and functional characterization. The synthetic approach should be appropriate to introduce non-natural amino acids at predetermined positions with a view to modifying either their selectivity or other pharmacological properties. This strategy was previously successfully applied to the engineering of modified toxins acting on voltage-dependent K^+ channels (Kalman et al., 1998; Alessandri-Haber et al., 1999).

Synthetic toxins sMT1 and sMT7 display physicochemical characteristics identical to those of the toxins purified from the mamba venom (vMT1) or recombinantly expressed (rMT7). As described previously, this rMT7 possesses biological activity identical to that of the venom's toxin (Nasman et al., 2000). The two toxin pairs, sMT1/vMT1 on the one hand and sMT7/rMT7 on the other, coeluted in reversed phase HPLC and have similar masses, confirming their identity. The CD spectra of synthetic toxins mostly consist of β-sheet secondary structure elements, suggesting that both toxins display a three-finger fold structure similar to that of MTX2 (Segalas et al., 1995). However, slight differences in their CD spectra may be the result, in the case of the sMT1, of a different distribution of the aromatic residues along the toxin sequence (see Fig. 1) (Drake et al., 1980). Therefore, we cannot exclude the possible occurrence of local weak structural deviations.

To ensure definitively that the synthetic muscarinic toxins display all the features of the venom's purified or recombinant toxins, we showed that their respective pharmacological properties were indistinguishable. First, the two synthetic toxins were tested on different muscarinic receptor subtypes by using CHO cells expressing the human M_1–M_4 receptors. sMT1 and vMT1 are characterized by similar apparent affinity constants of 20 and 35 nM for the M_1 receptor, whereas sMT1 interacts with the M_4 subtype with a 10-fold lower affinity (K_d = 340 nM). A 10 μM concentration of this toxin was unable to displace [^{3}H]NMS from M_2 and M_3 subtypes. The chemically synthesized (sMT7) or recombinant (rMT7) toxins [also called m1-toxin1 (Carsi and Potter, 2000)] were characterized, respectively, by IC_{50} values equal to 0.43 and 0.60 nM for the M_1 receptor. This toxin interacts with selectivity at least 20,000 times higher for the M_1 receptor compared with the other subtypes. All the values reported in Table 1 are in good agreement with previous affinities described in the literature (for review, see Bradley, 2000; Karlsson et al., 2000), confirming that the chemically synthesized toxins have pharmacological affinities and specificities

TABLE 1

Apparent affinity constants of wild-type and modified synthetic toxins sMT1 and sMT7 with various muscarinic receptor subtypes.

IC_{50} values were deduced from competition binding experiments and apparent affinity constants for the competitive sMT1 and sMT7-R34A interactions were calculated using the Cheng-Prusoff equation. Values are presented as mean ± S.E.M. (n = 3).

	hM_1		hM_2		hM_3		hM_4	
	IC_{50}	K_i	IC_{50}	K_i	IC_{50}	K_i	IC_{50}	K_i
	nM		*nM*		*nM*		*nM*	
sMT7	0.43 ± 0.04		>10,000		>10,000		>10,000	
rMT7	0.60 ± 0.11							
sMT1	315 ± 60	20 ± 4	>10,000		>10,000		5,500 ± 725	340 ± 45
vMT1	560 ± 140	35 ± 8						
sMT7-R34A	45 ± 8	7.5 ± 1.3						
sMT1-R34A	53,500 ± 14,000	3,315 ± 875						

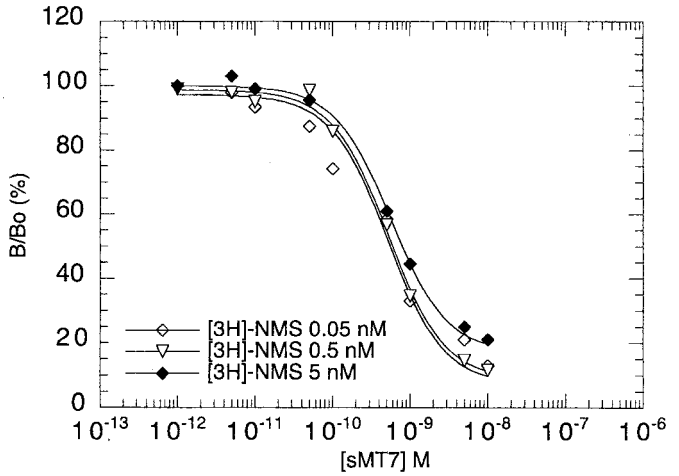

Fig. 6. Inhibition of specific [^{3}H]NMS binding to M_1 receptor by sMT7. Three different concentrations of [^{3}H]NMS were used (0.05, 0.5, and 5 nM) in the binding experiments. The results are expressed as the ratio of the specific [^{3}H]NMS binding measured with or without toxin (n = 3 at each [^{3}H]NMS concentration). The same experimental data were used for the competition at 0.5 nM of [^{3}H]NMS as in Fig. 5B.

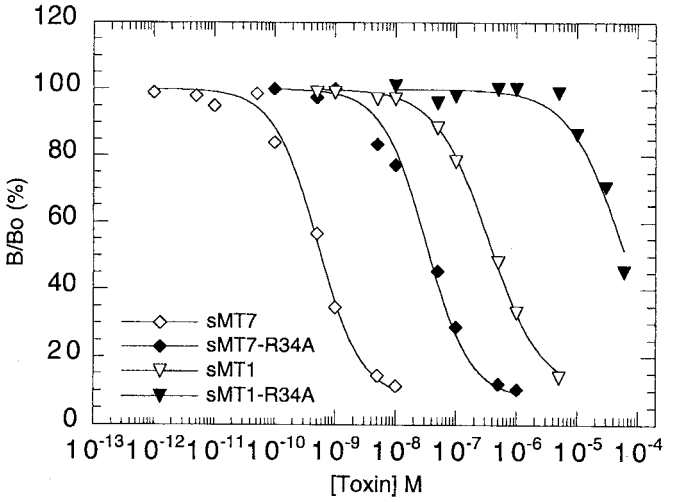

Fig. 7. Inhibition of the [^{3}H]NMS binding to human cloned M_1 muscarinic receptor by wild-type and R34A modified sMT1 and sMT7 toxins. Competition experiments were performed as described in Fig. 5. The same experimental data were used for the competition of sMT1 and sMT7 as in Fig. 5.

nearly identical to those of the natural toxins. The quasi-irreversible binding of sMT7 toxin to the M_1 receptor (Max et al., 1993; Carsi and Potter, 2000; Olianas et al., 2000) renders the calculation of its true affinity constant difficult, and the use of IC_{50} values is preferable. In addition, the large quantity of toxin available by chemical synthesis allowed testing for the first time of the effect of 10 μM sMT7 on the M_2–M_4 receptors, indicating that this toxin interacts preferentially (at least 10,000 times greater affinity) with the M_1 subtype.

Comparison of the functional properties and amino acid sequences of various muscarinic toxins allows us to propose the roles of different residues in their specific pharmacological profiles. For example, the 19 residues that differ in the sequences of sMT1 and sMT7 might explain their distinct modes of interaction with the M_1 receptor or their different selectivity profiles with various receptor subtypes. Highly conserved residues might be involved in the common process by which these toxins interact with the muscarinic receptor. The presence of conserved and variable residues at the site at which toxins from the same family interact with their targets was previously confirmed for the interactions of curaremimetic toxins with nicotinic receptors (Antil et al., 1999) and of sea anemone toxins with Kv1 channels (Alessandri-Haber et al., 1999; Racape et al., 2002; review in Ménez et al., 2002). To study whether the invariant positively charged residue at the tip of the central loop of all the muscarinic toxins might be part of a common binding site through which they interact with muscarinic receptors, we mutated the Arg-34 into an alanine in both toxin sequences. These mutations do not alter the overall structure of the toxins but induce in classic competition experiments 100- and 170-fold decreases in IC_{50} values in sMT7 and sMT1, respectively. Thus, as suggested previously, the protruding positive side chain at the tip of the central loop was involved in the binding of muscarinic toxins

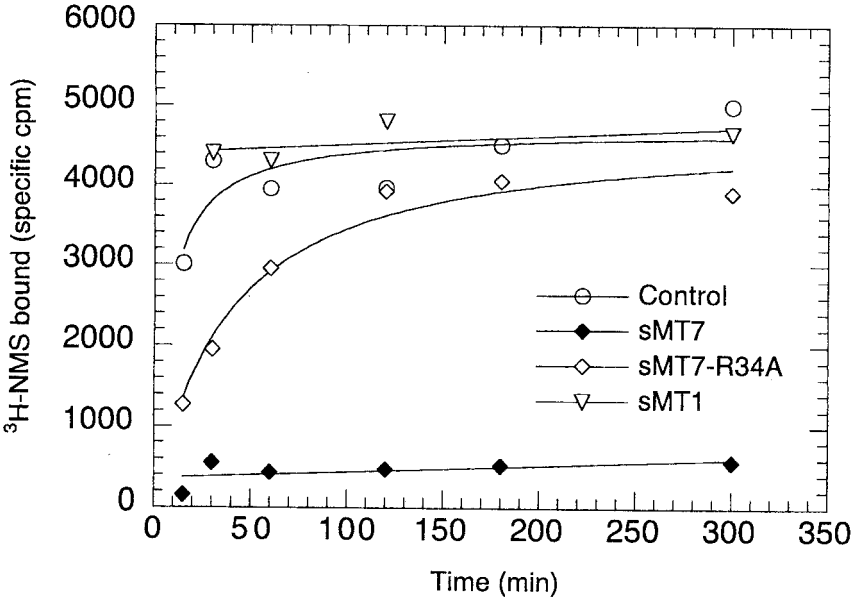

Fig. 8. Stability of the inhibition of [^{3}H]NMS binding to the M_1 receptor by sMT1, sMT7, and sMT7-R34A. hM1 membranes were incubated first with a saturating concentration of toxins, sMT7 (10 nM), sMT7-R34A (1 μM), and sMT1 (5 μM) and then with [^{3}H]NMS (1 nM). In the control experiments, no toxin was added. The rate of appearance of binding sites for [^{3}H]NMS was taken as the rate of dissociation of the different toxins. Data are the results of one experiment that was repeated three times.

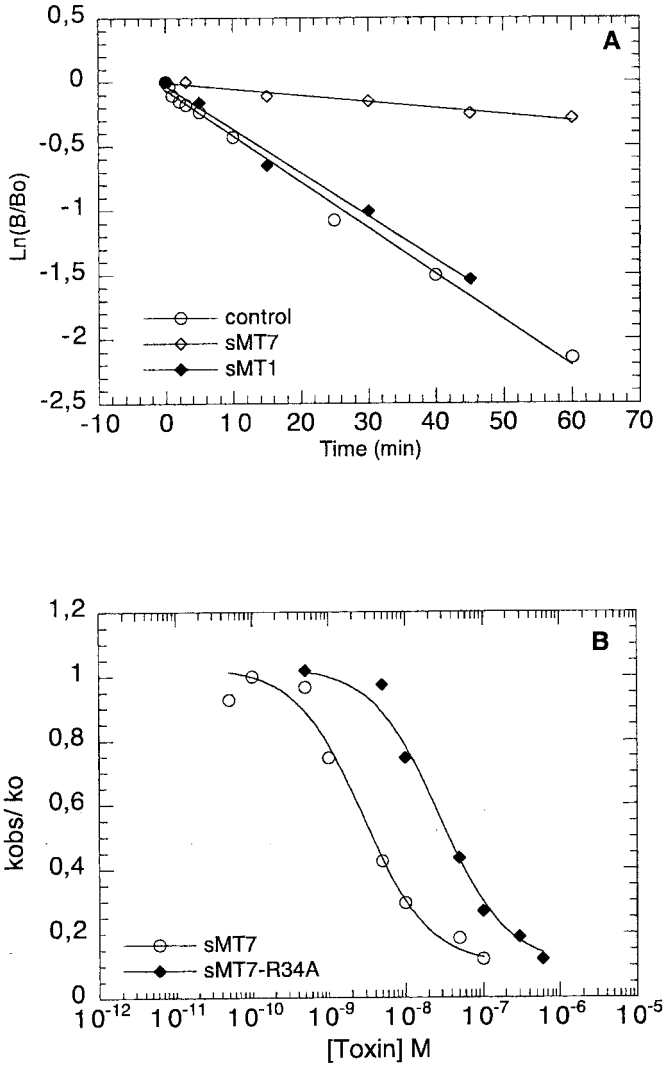

Fig. 9. Variation of the atropine-induced [^{3}H]NMS dissociation from the M_1 receptor in the presence of wild-type or modified toxins. A, M_1 receptor cell membranes were incubated with 1 nM [^{3}H]NMS for 45 min and dissociation of the radioligand was initiated by the addition of 3 μM atropine, with or without sMT7 (20 nM) or sMT1 (40 μM). [^{3}H]NMS dissociation was expressed on a semilogarithmic scale, where *B* and *Bo* represent the specific binding at time *t* or *t*0, respectively. B, inhibition of the [^{3}H]NMS dissociation by various concentrations of sMT7 and sMT7-R34A using the single time point determination as described under *Materials and Methods*. The apparent rate constants for the dissociation of [^{3}H]NMS were determined in the presence of each concentration of toxins (k_{obs}) and divided by the true rate constant k_o determined in the presence of atropine only. Data are the results of one experiment that was repeated three times.

to their receptors (Segalas et al., 1995). It may be noticed that, among the other three-finger toxins, the curaremimetic toxins also present a conserved Arg residue in a similar position. Interestingly, this residue has been shown to belong to the toxic site of these toxins when interacting with muscular (Trémeau et al., 1995; Antil et al., 1999; Rosenthal et al., 1999) or neuronal (Fiordalisi et al., 1994; Antil-Delbeke et al., 2000) nicotinic acetylcholine receptors. Recently, a structural model of the latter interaction confirmed the importance of this cationic group (Fruchart-Gaillard et al., 2002). To characterize further the type of interaction of these two toxins, their effect on the stability of the [^{3}H]NMS binding to M_1 receptor was studied. In agreement with previous results, sMT1 was found to bind reversibly to the M_1 receptor (Waelbroeck et al., 1996). In contrast, sMT7 blocks [^{3}H]NMS binding for at least 5 h, confirming its quasi-irreversible binding (Max et al., 1993; Olianas et al., 2000; Krajewski et al., 2001). In addition, we demonstrate that the R34A modification significantly affects the irreversibility of the sMT7-M_1 receptor interaction. Thus, because of the reversible interaction of sMT7-R34A on the M_1 receptor, a Cheng-Prusoff correction could be applied to the inhibition data shown in Fig. 7, conducing to an apparent affinity constant equal to 7.5 nM (Table 1). Nevertheless, the critical role of this residue in the MT7 binding is still confirmed, especially if we assume that the IC_{50} for sMT7 binding is a gross overestimate of its intrinsic potency given that its binding is pseudo-irreversible.

Furthermore, the effect of sMT1 and sMT7 on the atropine-induced [^{3}H]NMS dissociation from the M_1 receptor was investigated. It was found that, even at high concentration (40 μM), sMT1 had no significant effect on the [^{3}H]NMS dissociation rate, suggesting that this toxin interacts not with the allosteric site but more probably with the orthosteric site. This result agrees well with previous reports on the pharmacological and functional properties of MT1 (Jerusalinsky and Harvey, 1994; Waelbroeck et al., 1996; Jerusalinsky et al., 2000), even if conflicting data on the MT1 binding site are reported (Jerusalinsky et al., 1995). Nevertheless, we cannot conclude definitively on the binding of MT1 to the orthosteric site, because a high degree of negative cooperativity is indistinguishable from a competition interaction. sMT7 decreases the [^{3}H]NMS dissociation 7-fold, in agreement with other results confirming the ability of this toxin to interact at the allosteric site of the M_1 receptor (Olianas et al., 2000; Krajewski et al., 2001). This property is confirmed by competition experiments with sMT7 and increasing concentrations of [^{3}H]NMS leading to quasi-identical IC_{50} values associated with slope factors greater than 1. Finally, the apparent affinity constants of wild-type and modified sMT7 for the [^{3}H]NMS-liganded receptor were determined. The R34A modification induces a 10-fold decrease in the toxin IC_{50} value, confirming the role of Arg-34 residue in the interaction of sMT7 at the receptor allosteric binding site. The differences observed in the potencies of sMT7 and sMT7-R34A, determined, respectively, in equilibrium binding (0.43 and 7.5 nM) and dissociation experiments (2.5 and 24 nM), might be explained in terms of allosteric interaction, by a negative cooperativity between the wild-type or modified toxins and the prebound NMS.

The putative competitive binding of sMT1 to the M_1 receptor and the critical role of its Arg-34 may suggest that the tip of the central toxin loop plugs into the transmembrane domains of the receptor, to reach the agonist-binding pocket. On the other hand, the possible interaction of sMT7 with a receptor-antagonist complex suggests that this toxin might act by modulating accessibility to the orthosteric site by interacting with the extracellular face of the receptor. Nevertheless, even in this case, the Arg-34 seems important in this interacting process. Because the positively charged Arg-34 seems critical in the binding of sMT1 and sMT7 toxins to muscarinic receptors, we would like to examine whether their remaining charged residues participate in their various modes of interaction with the M_1 receptor. Supporting this hypothesis, a close inspection of toxin sequences (Fig. 1)

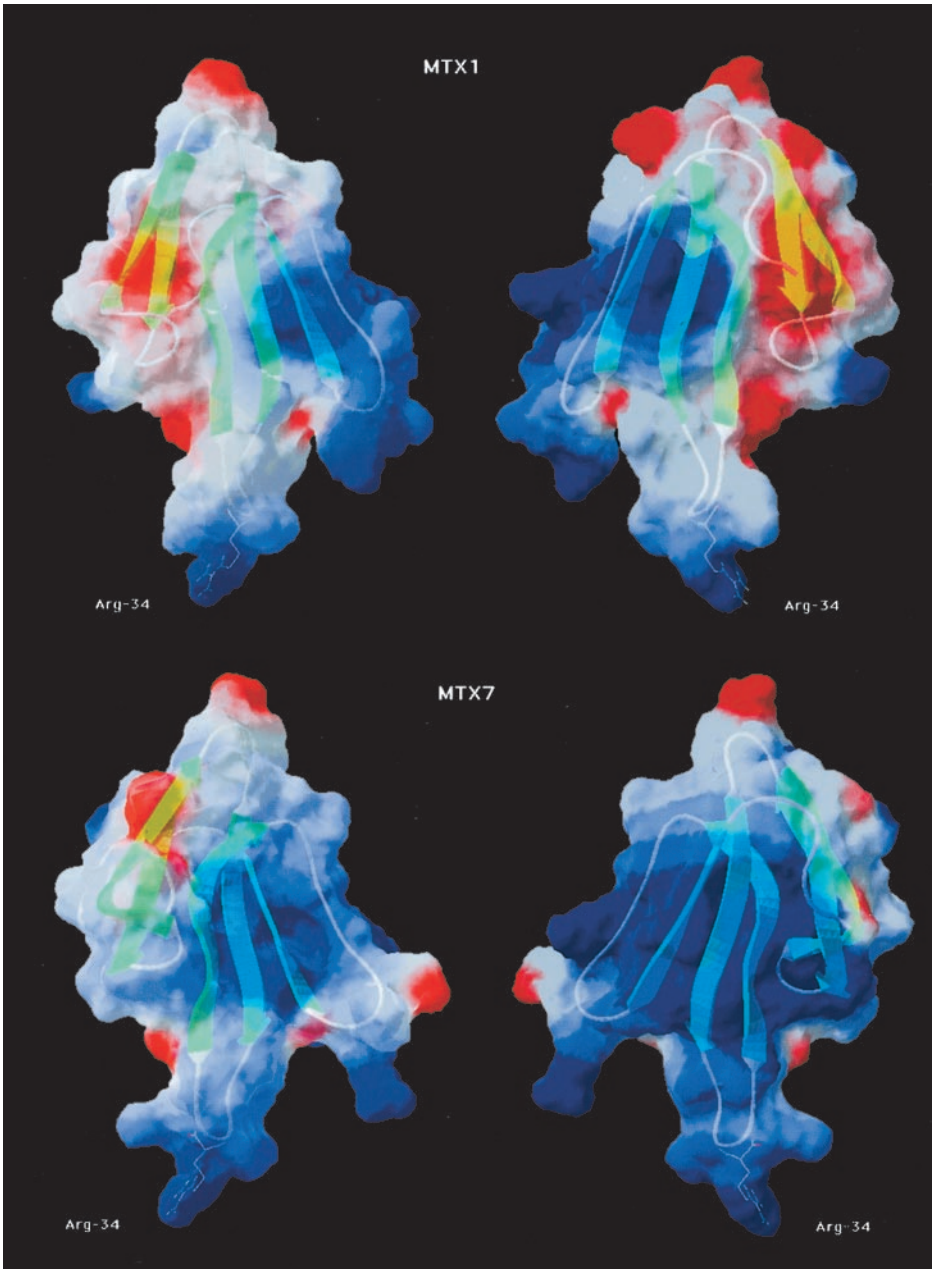

Fig. 10. Electrostatic surface potential representations of sMT1 (top) and sMT7 (bottom) toxins, viewed from their concave (left) and convex (right) faces. The 3D models of the two toxins were obtained with the Swiss-PdbViewer and Swiss Model programs, starting from the NMR structure of the MTX2. The location of the critical Arg-34 side chain is indicated at the tip of the toxin loop 2 and positive, negative, and hydrophobic regions are colored in blue, red and white, respectively.

indicates that seven charged residues are differently located. We therefore modeled the 3D structure of both toxins starting from the NMR structure of MTX2 (Segalas et al., 1995) and compared their respective calculated electrostatic potentials. The four views of the molecular surface of MT1 and MT7 (Fig. 10) highlight the difference in charge distribution in the two toxins. Thus, whereas some conserved charged residues are identically positioned in MT1 and MT7 (Asp-19, Arg-34, Arg-53), the global charge distribution is quite different. MT7 toxin seems predominantly positively charged on its two faces, whereas MT1 possesses large electronegative patches on its convex and concave faces, mainly supported by C-terminal residues (Fig. 10). The variation in the distribution of surface charge between the two toxins might explain, at least partially, the different ways in which they bind to the same M_1 receptor. Mutant-cycle experiments, using toxin and receptor mutants, should be a good way to test this hypothesis and to propose, as with the interaction of a three-finger fold toxin with the nicotinic receptor (Fruchart-Gaillard et al., 2002), a structural model of toxin-muscarinic receptor interactions.

Acknowledgments

We thank Prof. P. O. Couraud and Prof. A. D. Strosberg (ICGM, Paris, France) for the gift of CHO cells expressing M_1–M_4 muscarinic receptors and Dr. E. Karlsson (Department of Clinical Neuroscience, Karolinska Institute, Huddinge, Sweeden) for the gift of recombinant

MT7. We are grateful to A. Michaud and L. Pinto for their technical assistance.

References

Adem A and Karlsson E (1997) Muscarinic receptor subtype selective toxins. *Life Sci* **60:**1069–1076.

Alessandri-Haber N, Lecoq A, Gasparini S, Grangier-Macmath G, Jacquet G, Harvey AL, de Medeiros C, Rowan EG, Gola M, Ménez A, et al. (1999) Mapping the functional anatomy of BgK on Kv1.1, Kv1.2 and Kv1.3. Clues to design analogs with enhanced selectivity. *J Biol Chem* **274:**35653–35659.

Altschul SF, Madden TL, Schäffer AA, Zhang J, Zhang Z, Miller W, and Lipman DJ (1997) Gapped BLAST and PSI-BLAST: a new generation of protein database search programs. *Nucleic Acids Res* **25:**3389–3402.

Antil S, Servent D, and Ménez A (1999) Variability among the sites by which curaremimetic toxins bind to *Torpedo* acetylcholine receptor, as revealed by identification of the functional residues of α-cobratoxin. *J Biol Chem* **274:**34851–34858.

Antil-Delbeke S, Gaillard C, Tamiya T, Corringer PJ, Changeux JP, Servent D, and Ménez A (2000) Molecular determinants by which a long chain toxin from snake venom interacts with the neuronal α7 nicotinic acetylcholine receptor. *J Biol Chem* **275:**29594–29601.

Bradley KN (2000) Muscarinic toxins from the green mamba. *Pharmacol Ther* **85:**87–109.

Carpino LA, El-Farham A, Minor C, and Albericio F (1994) Advantageous application to azabenzotriazole-based coupling reagents to solid-phase peptide synthesis. *J Chem Soc Chem Commun* 201–206.

Carsi JM and Potter LT (2000) m1-toxin isotoxins from the green mamba (Dendroaspis angusticeps) that selectively block m1 muscarinic receptors. *Toxicon* **38:**187–198.

Cheng Y-C and Prusoff WH (1973) Relationship between the inhibition constant (Ki) and the concentration of inhibitor which causes 50 per cent inhibition (I50) of an enzymatic reaction. *Biochem Pharmacol* **22:**3099–3108.

Drake AF, Dufton MJ, and Hider RC (1980) Circular dichroism of elapidae protein toxins. *Eur J Biochem* **105:**623–630.

Eglen RM, Choppin A, Dillon MP, and Hegde S (1999) Muscarinic receptor ligands and their therapeutic potential. *Curr Opin Chem Biol* **3:**426–432.

Ellis J and Seidenberg M (2000) Interactions of alcuronium, TMB-8 and other allosteric ligands with muscarinic acetylcholine receptors: studies with chimeric receptors. *Mol Pharmacol* **58:**1451–1460.

Fiordalisi JJ, al-Rabiee R, Chiappinelli VA, and Grant GA. (1994) Site-directed mutagenesis of κ-bungarotoxin: implications for neuronal receptor specificity. *Biochemistry* **33:**3872–3877.

Fruchart-Gaillard C, Gilquin B, Antil-Delbeke S, Le Novère N, Tamiya T, Corringer PJ, Changeux JP, Ménez A, and Servent D (2002) Experimentally-based model of a complex between a snake toxin and the α7 nicotinic acetylcholine receptor. *Proc Natl Acad Sci USA* **99:**3216–3221.

Gnagey AL, Seidenberg M, and Ellis J (1999) Site-directed mutagenesis reveals two epitopes involved in the subtype selectivity of the allosteric interactions of gallamine at muscarinic acetylcholine receptors. *Mol Pharmacol* **56:**1245–1253.

Guex N and Peitsch MC (1997) SWISS-MODEL and the Swiss-PdbViewer: an environment for comparative protein modelling. *Electrophoresis* **18:**2714–2723.

Jerusalinsky D and Harvey AL (1994) Toxins from mamba venoms: small proteins with selectivities for different subtypes of muscarinic acetylcholine receptors. *Trends Pharmacol Sci* **15:**424–430.

Jerusalinsky D, Kornisiuk E, Alfaro P, Quillfeldt J, Ferreira A, Rial VE, Duran R, and Cervenansky C (2000) Muscarinic toxins: novel pharmacological tools for the muscarinic cholinergic system. *Toxicon* **38:**747–761.

Jerusalinsky D, Kornisiuk E, Bernabeu R, Izquierdo I, and Cervenansky C (1995) Muscarinic toxins from the venom of Dendroaspis snakes with agonist-like actions. *Toxicon* **33:**389–397.

Kalman K, Pennington MW, Lanigan MD, Nguyen A, Rauer H, Mahnir V, Paschetto K, Kem WR, Grissmer S, Gutman GA, et al. (1998) ShK-Dap22, a potent Kv1.3-specific immunosuppressive polypeptide. *J Biol Chem* **273:**32697–32707.

Karlsson E, Jolkonen M, Mulugeta E, Onali P, and Adem A (2000) Snake toxins with high selectivity for subtypes of muscarinic acetylcholine receptors. *Biochimie* **82:**793–806.

Krajewski JL, Dickerson IM, and Potter LT (2001) Site-directed mutagenesis of m1-toxin1: two amino acids responsible for stable toxin binding to M_1 muscarinic receptors. *Mol Pharmacol* **60:**725–731.

Lazareno S, Popham A, and Birdsall NJ (2000) Allosteric interactions of staurosporine and other indolocarbazoles with *N*-[methyl-^{3}H]scopolamine and acetylcholine at muscarinic receptor subtypes: identification of a second allosteric site. *Mol Pharmacol* **58:**194–207.

Max SI, Liang JS, and Potter LT (1993) Stable allosteric binding of m1-toxin to m1 muscarinic receptors. *Mol Pharmacol* **44:**1171–1175.

Ménez A (1998) Functional architectures of animal toxins: a clue to drug design? *Toxicon* **36:**1557–1572.

Ménez A, Servent D, and Gasparini S (2002) The sites by which animal toxins bind to their targets involve two components: a clue for selectivity, evolution and design of proteins, in *Perspectives in Molecular Toxinology* (Ménez A ed) pp 175–202, John Wiley & Sons, Ltd., New York.

Mourier G, Servent D, Zinn-Justin S, and Ménez A (2000) Chemical engineering of a three-fingered toxin with anti-α7 neuronal acetylcholine receptor activity. *Protein Engineering* **13:**217–225.

Nasman J, Jolkkonen M, Ammoun S, Karlsson E, and Akerman KE (2000) Recombinant expression of a selective blocker of M_1 muscarinic receptors. *Biochem Biophys Res Commun* **271:**435–439.

Nishiuchi Y, Nishio H, Inui T, Bodi J, and Kimura T (2000) Combined solid-phase and solution approach for the synthesis of large peptides or proteins. *J Pept Sci* **6:**84–93.

Olianas MC, Maullu C, Adem A, Mulugeta E, Karlsson E, and Onali P (2000) Inhibition of acetylcholine muscarinic M(1) receptor function by the M(1)-selective ligand muscarinic toxin 7 (MT-7). *Br J Pharmacol* **131:**447–452.

Peitsch MC (1995) Protein modeling by E-mail. *Biotechnology* **13:**658–660.

Peitsch MC (1996) ProMod and Swiss-Model: internet-based tools for automated comparative protein modelling. *Biochem Soc Trans* **24**:274–279.

Potter LT (2001) Snake toxins that bind specifically to individual subtypes of muscarinic receptors. *Life Sci* **68,** 2541–2547.

Racape J, Lecoq A, Romi-Lebrun R, Liu J, Kohler M, Garcia ML, Ménez A, and Gasparini S (2002) Characterization of a novel radiolabeled peptide selective for a subpopulation of voltage-gated potassium channels in mammalian brain. *J Biol Chem* **277:**3886–3893.

Rosenthal JA, Levandoski MM, Chang B, Potts JF, Shi Q-L, and Hawrot E (1999) The functional role of positively charged amino acid side chains in α-bungarotoxin revealed by site-directed mutagenesis of a His-tagged recombinant α-bungarotoxin. *Biochemistry* **38:**7847–7855.

Segalas I, Roumestand C, Zinn-Justin S, Gilquin B, Menez R, Menez A, and Toma F (1995) Solution structure of a green mamba toxin that activates muscarinic acetylcholine receptors, as studied by nuclear magnetic resonance and molecular modeling. *Biochemistry* **34:**1248–1260.

Thompson JD, Higgins DG, and Gibson TJ (1994) CLUSTAL W: improving the sensitivity of progressive multiple sequence alignment through sequence weighting, position-specific gap penalties and weight matrix choice. *Nucleic Acids Res* **22:**4673–4680.

Trémeau O, Lemaire C, Drevet P, Pinkasfeld S, Ducancel F, Boulain JC, and Ménez A (1995) Genetic engineering of snake toxins. The functional site of Erabutoxin a, as delineated by site-directed mutagenesis, includes variant residues. *J Biol Chem* **270:**9362–9369.

Waelbroeck M, De Neef P, Domenach V, Vandermeers-Piret MC, and Vandermeers A (1996) Binding of the labelled muscarinic toxin 125I-MT1 to rat brain muscarinic M1 receptors. *Eur J Pharmacol* **305:**187–192.

Address correspondence to: Denis Servent, CEA, Département d'Ingénierie et d'Etude des Protéines, 91191 Gif-sur-Yvette, France. E-mail: denis.servent@cea.fr